Spectral negative refraction and focusing analysis of a two-dimensional left-handed photonic crystal lens

K. Guven,[1,*] K. Aydin,[1] K. B. Alici,[1] C. M. Soukoulis,[2] and E. Ozbay[1,3]
[1]*Department of Physics, Bilkent University, Bilkent, 06800 Ankara, Turkey*
[2]*Ames Laboratory-USDOE and Department of Physics and Astronomy, Iowa State University, Ames, Iowa 50011, USA*
[3]*Advanced Research Laboratory, Bilkent University, Bilkent, 06800, Ankara, Turkey*
(Received 28 June 2004; revised manuscript received 17 September 2004; published 22 November 2004)

We report the spectral refraction analysis and focusing properties of a two-dimensional, dielectric photonic crystal (PC) slab in freespace. A transverse electric polarized upper band of the crystal is used. The measured refraction spectra indicates that a highly isotropic negative index of refraction is present in the measured frequency range of the band. We demonstrate experimentally and numerically the focusing of the field emitted from an omnidirectional source placed in front of the crystal. Both the source and the focus pattern are away from the PC interfaces of the order of several wavelengths. The focus pattern mimics the arbitrary lateral and longitudinal shifts of the source, which is a manifestation of true flat lens behavior.

DOI: 10.1103/PhysRevB.70.205125 PACS number(s): 42.25.−p, 78.20.Ci, 42.79.Bh

I. INTRODUCTION

Photonic crystals (PCs) are making profound changes to the way we control the propagation of light.[1] These periodically (or quasi-periodically) modulated dielectric or metallic structures provide bands for the photons in close analogy to the bands of electrons in a semiconductor material, hence the name "photonic crystal." By tuning the geometrical and material parameters of the crystal, the band structure can be sculptured to yield virtually any type of dispersion for the propagation of electromagnetic waves, which reveals novel and unusual optical phenomena.[2–11] An exciting feature among these is the negative refraction of electromagnetic waves at the interface between a positive index medium (e.g., air) and the PC.[2–7,9,11] This, and the large beam steering, called "super prism phenomenon," at the interface of a three-dimensional (3D) PC has been experimentally observed by Kosaka *et al.*[2] Theoretical studies indicate that the underlying mechanism for the negative refraction in PCs is not unique: Notomi extensively studied and light propagation and described different ways for achieving negative effective index of refraction, n_{eff}, in strongly modulated two-dimensional (2D) PCs.[4] Negative refraction may occur when the incident field couples to a band with convex equal frequency contours (EFCs) in **k**-space, where the conservation of the surface parallel component of the wavevector, **k**, combined with the "negative" curvature of the band causes the incident beam bend negatively.[4,5] In this case, neither the group velocity nor the effective index is negative and the PC is essentially a positive index medium, exhibiting negative refraction. In another mechanism, the group velocity and the phase velocity derived from the band dispersion are antiparallel for all the values of **k**, leading to $n_{\text{eff}}<0$ for the PC.[6] Both mechanisms are confirmed by recent experimental observations.[8,9,11] Negative refraction studies originate from left handed metamaterials[12,13] which are based on the proposal by Veselago,[14] composed from periodically arranged negative permeability ($\mu<0$) and permittivity ($\varepsilon<0$) metal components, providing an effective medium with $n=\sqrt{\varepsilon}\sqrt{\mu}<0$.

The interest in negative refraction phenomenon does not stem only from fundamental physics point of view. Pendry[15] proposed that negative n_{eff} in left-handed materials can be used for constructing a perfect lens, which may not be limited by diffraction. Luo *et al.* studied the subwavelength imaging in PCs in detail.[16] Cubukcu[8] *et al.* demonstrated experimentally the subwavelength resolution along a 2D PC-air interface. Recently, Parimi[10] *et al.* demonstrated the near field image formation of a point source with a 2D PC and negative refraction in a 2D metallic PC prism.[11] The focusing properties of a rectangular dielectric photonic crystal lens were also studied experimentally and by simulations by Martinez *et al.*[17]

In this article, we present the spectral negative refraction analysis and focusing properties of a 2D photonic crystal slab. Our achievements in a nutshell are that: (1) Unlike previous experimental studies, a transverse electric (TE) polarized upper band of the crystal is utilized; (2) the band is shown to exhibit an isotropic refraction to certain extend, with high transmission (~ -4 dB compared to free-space propagation); (3) the focusing of the transmitted field is obtained *far away* from the crystal interface with a resolution on par with the wavelength and a high transmission level; (4) strong evidence is found for true flat lens behavior of the PC.

II. SPECTRAL NEGATIVE REFRACTION ANALYSIS OF A 2D PHOTONIC CRYSTAL

We follow the analysis presented in Ref. 6 to obtain a PC with negative n_{eff}. The photonic crystal is a hexagonal lattice of alumina rods in air. Lattice period is $a=4.79$ mm. The rods have dielectric constant $\varepsilon=9.61$, diameter $2r=3.15$ mm, and length $l=15$ cm. The top part of Fig. 1 displays the transverse electric (TE) polarized band structure in the first Brillouin zone. Throughout this paper, the transverse direction is taken in plane of the 2D photonic crystal. The 5th band shaded in the figure extends from $\tilde{f}=0.65$ ($f=40.65$ GHz) to $\tilde{f}=0.74$ ($f=46.27$ GHz), where $\tilde{f}=fa/c$ is

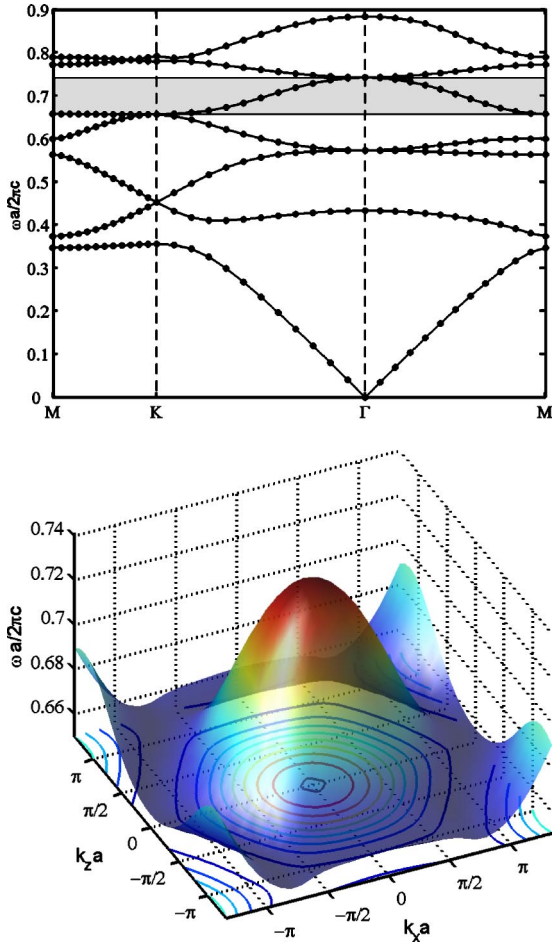

FIG. 1. (Color online) (top) TE polarized band structure of the PC. 5th band (shaded) gives negative refraction. (bottom) The surface (transparent shell) of the 5th band in the full Brillouin zone. Some equal frequency contours are projected to the Brillouin zone plane.

the scaled frequency. In the bottom part of Fig. 1, the band surface in the full Brilloin zone along with the projected equal-frequency contours (EFCs) are shown. The EFCs of the band are shrinking with increasing frequency, contrary to the EFCs in air ($n=1$) which are given by the dispersion $\omega=ck$. As a result, the effective refractive index $n_p=\mathrm{sgn}(\vec{v}_g\cdot\vec{k}_f)(c|\vec{k}_f|/\omega)$, becomes negative due to sign of the antiparallel group velocity $\vec{v}_g=\nabla_{\vec{k}}\omega$ and the phase velocity $\vec{v}_p=(c/|n_p|)\hat{k}_f$. Here c is the speed of light in vacuum, and $\hat{k}_f$ is the unit wavevector in the PC. We note that the EFC starts to deviate from the circular shape towards the bottom edge of the band, which will induce some anisotropy. We discuss this effect later.

The refraction spectra are measured by a setup consisting of an HP 8510C network analyzer, a microwave horn antenna as the transmitter and a waveguide antenna as the receiver. Figure 2 displays the schematic view of the setup. The PC has 7 layers along the incidence (ΓM) direction and 31 layers along the lateral direction. The horn antenna is on the negative side of the PC with respect to its central axis. The spatial intensity distribution along the PC-air interface is

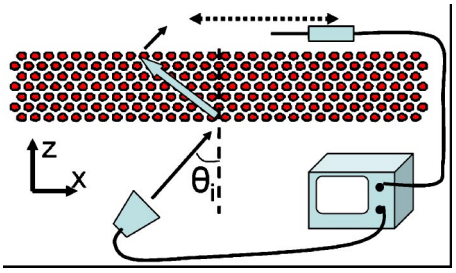

FIG. 2. (Color online) Schematic of the refraction spectra measurement setup. The EM wave is emitted from a horn antenna, incident to the PC at θ_i. The lateral intensity distribution of the refracted beam at the other interface is scanned by a monopole antenna. An HP8510C network analyzer is used to obtain the transmission spectra.

scanned by $\Delta x\sim 1.27$ mm steps, while the frequency is swept from 38.5 to 43.5 GHz in 400 steps, averaged over 256 measurements at each frequency.

Figure 3(a) displays the transmission spectra as a function of frequency and lateral position for three different incidence angles of $\theta_i=15°$, 30°, and 45°. It is evident that the transmitted beam appears on the negative side. When the incidence angle is increased the transmission shifts towards left accordingly. To investigate the beam profiles, the spatial cross section at $f=41.7$ GHz ($\tilde{f}=0.667$) are plotted in Fig. 3(b). We note that the incident field has a Gaussian beam profile centered at $x=0$ (not shown on figures). The intensities are normalized with respect to the maximum intensity for the 15° incidence. The lateral shift is accompanied by a decrease in the transmission intensity. This can be attributed to the higher reflection at the interface for larger incidence angles and to the diffraction induced out-of-plane losses which increase with increasing path through the lattice. Figure 3(c) displays the corresponding profiles obtained from FDTD simulations which show very good agreement to experimental profiles.

Before we commence an effective index of refraction calculation using the measured and simulated refraction data, visualizing the field distribution by an FDTD simulation may help to gain insight about the presence/absence of higher order reflected and refracted wave components. Figure 4 depicts a simulation for the $\theta_i=30°$ incidence. Evidently, higher order reflection (mark 3) is present because at $\tilde{f}=0.667$ the condition $\tilde{f}\leqslant a/(2a_{\mathrm{interface}})$ is not met,[5,18] where $a_{\mathrm{interface}}$ is the interface period of the PC. The refracted beam, however, appears to be a single component, which is also suggested by the single transmitted component on the other side of the PC. One may argue that the simulation at $\theta_i=30°$ is not conclusive as the surface parallel wavevector changes with incidence angle. This is indeed the case, but the simulations of the present structure indicate that the a single refracted beam is present for incidence angles $\theta_i\leqslant 45°$. Both Notomi,[4] as well as Foteinopoulou and Soukoulis[7,18] pointed out that single beam refraction at higher bands is possible. We, therefore, assume that most of the propagating power is coupled to the zero-order diffracted wave, and employ Snell's law for this geometry by $n(f,k_i)\sin\theta_f=n_{\mathrm{air}}\sin\theta_i$, where θ_i is the

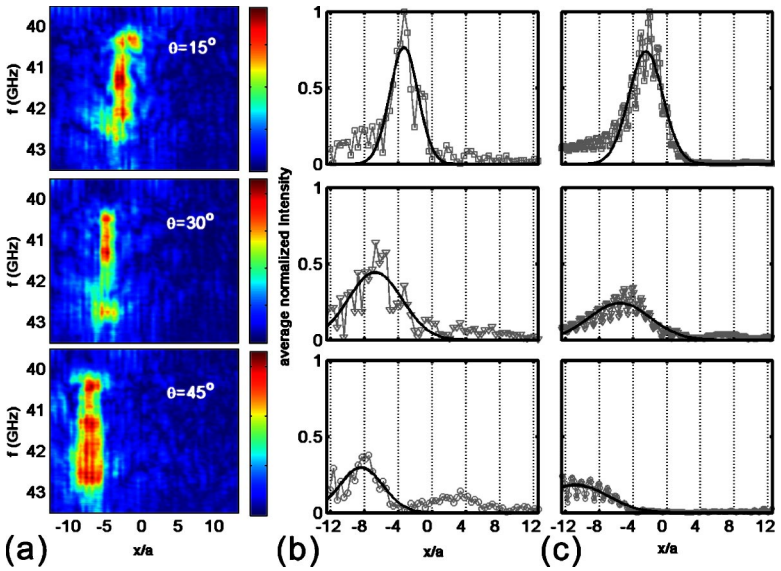

FIG. 3. (Color online) (a) Measured negative refraction spectra of the 5th band along the PC-air interface for incidence angles $\theta=15°$, 30°, and 45°. Measured (b) and simulated (c) intensity profiles at $f=41.7$ GHz for the respective incidence angles. Solid curves indicate Gaussian fits.

angle of incidence and θ_f is the angle of refraction inside the photonic crystal. For $\theta_i=15°$, 30°, and 45° we obtain $n_{\text{eff}}=-0.52$, -0.66, and -0.86 from the experiment, respectively. The simulation results for the same incidence angles give $n_{\text{eff}}=-0.66$, -0.72, and -0.80, respectively.

In general, n_{eff} depends both on the parallel component of the wavevector (i.e., angle of incidence) and the frequency of the field: $n_{\text{eff}}(\boldsymbol{k},\omega)$. The refraction spectra in Fig. 3 exhibits both dependencies to certain extend. The k-dependent anisotropy is apparent from the numerical values of n_{eff} obtained by applying Snell's Law. The frequency 41.7 GHz for which the lateral beam profiles are plotted is rather close to the lower edge of the band, which makes this anisotropy more prominent. As mentioned, increasing the parallel component of the wavevector may also induce higher order reflection and refraction at the interface. Although the frequency dependence of n_{eff} appears to be more subtle in the refraction spectra, we stress that the frequency range (40.65–43 GHz) plotted in Fig. 3 covers only the lower half of the band. The range above 43 GHz was beyond the limits of our measurement setup. Our conclusion is that the frequency dependent anisotropy occurring in this frequency range is not sufficient to reflect itself in the displayed spectra, in view of the width of the lateral beam profile as shown in Figs. 3(b) and 3(c). It is evident that the effective index of refraction of the band should change with frequency since it should approach to zero at the upper band edge. For an isotropic behavior in frequency, the dispersion of the band should be linear as in air medium (i.e., $w=c|\mathbf{k}|$), which is clearly not the case as can be seen on the band structure in Fig. 1. Despite the presence of the anisotropy, the band still manages to provide a uniform beam within the measured frequency range. Based on this behaviour, we discuss the response of the photonic crystal slab to a point-source in the next section.

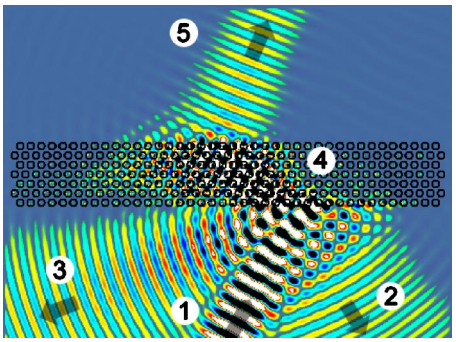

FIG. 4. (Color online) Simulated negative refraction of a plane wave at $f=41.7$ GHz incident at $\theta=30°$ to the PC interface (mark 1). Zero order (mark 2) and higher order (mark 3) reflections occur. The refracted (mark 4) the transmitted (mark 5) components appear to propagate as single beams.

III. FOCUSING PROPERTIES AND FLAT LENS BEHAVIOR OF THE 2D PHOTONIC CRYSTAL

The presence of negative refraction for large range of incidence angles brings the possibility that the slab structure may act like a lens for an omni-directional source. Theoretical studies predicted that a lens with negative n_{eff} may exhibit unusual focusing properties that surpass the limitations of its positive n_{eff} counterpart[15,16] and indeed such behavior is demonstrated.[8,10] For the present PC, we first performed FDTD simulations for a TE polarized point source at $f=42.07$ GHz located at a distance $d_{\text{src}}=2\lambda$ away from air-PC interface. Previous studies considered the case where the source is located in the vicinity of the PC interface ($d_{\text{src}}<\lambda$). Figure 5(b) shows the resulting spatial intensity distribution in the image plane, normalized by the maximum intensity value. The PC-air interface is located at $z=0$. The peak indicates focusing behavior unambiguously (we also refer the reader to Fig. 7 for the simulated 2D H-field map, where the convergence of the wavefronts along the optical axis is clearly visible). We would like to emphasize that the focusing occurs away from the PC-air interface, observed at $z\approx 8\lambda$. In this respect, channelling induced focusing effects may also be excluded, which occur close to the interface.[19]

In the experiment, a waveguide aperture is used as the source. Since the EM wave diffracts rapidly at the abrupt end

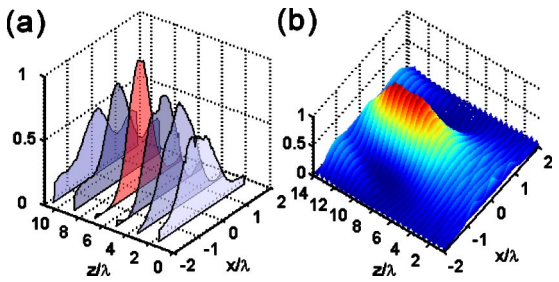

FIG. 5. (Color online) (a) Lateral intensity profiles measured at six different positions along the propagation direction: $z/\lambda=1.78$, 3.56, 5.34, 7.12, 8.90, and 10.68. $z=0$ corresponds to the PC interface (b) Simulated 2D intensity in the image plane.

of an waveguide aperture, we expect that the waveguide aperture provides sufficiently omnidirectional radiation to imitate a TE polarized true monopole (or monoloop) antenna for our purposes. The details of the radiation pattern does not impose any restrictions on the general properties of the focusing effect. The intensity distribution in the focusing plane is measured by a monopole antenna. For $d_{\mathrm{src}}=2\lambda$, first the propagation direction, z, is scanned for locating the maximum intensity, and then lateral cross sections of intensity at several z around the peak position are measured. In Fig. 5(a), the focusing of the beam both in lateral and longitudinal directions is evident. The maximum intensity (normalized to unity) is observed at $d_{\mathrm{focus}}/\lambda\approx 8$. The longitudinal extend the focusing indicates that n_{eff} deviates from negative unity, and has certain amount of anisotropy. As a result, the focus pattern cannot be regarded as an image formation in a strict sense. We further note that even when n_{eff} were perfectly isotropic and uniform, a value different than -1 would not generate point focusing and induce an aberration of the image.

The flat lens behavior of the PC structures was emphasized in recent studies.[10] In this case, the focusing properties are preserved at an arbitrary lateral location of the source along the interface. To demonstrate this, we have shifted the source laterally and measured the lateral beam profile at the

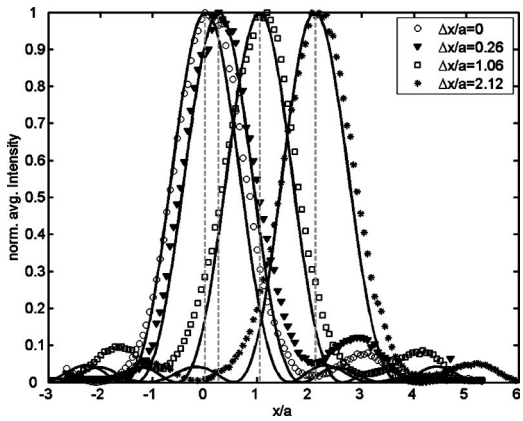

FIG. 6. The measured (symbols) and simulated (solid curves) lateral intensity profiles at the focal distance ($z/\lambda\approx 8$) for different lateral shifts. The respective source locations are denoted by vertical dashed lines.

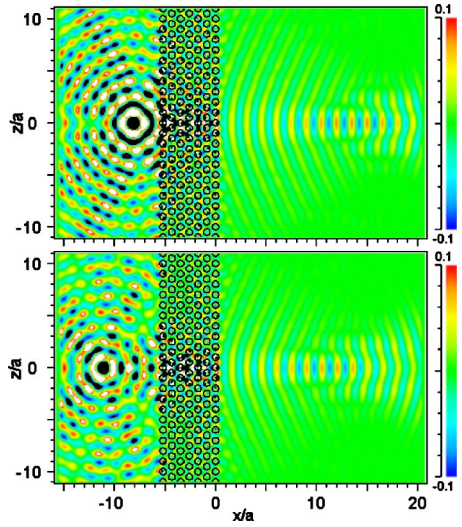

FIG. 7. (Color online) Simulated 2D field distribution $H_y(x,z)$ for $d_{\mathrm{src}}=2\lambda$ (top) and $d_{\mathrm{src}}=4\lambda$ (bottom).

focal point. As seen in Fig. 6, the source positions (vertical dashed lines) and the peak positions of the focused beam (symbols) are in excellent agreement. In addition, the simulated profiles (solid curves) using a true point source show a remarkable match with the measured data. We, therefore, conclude that for d_{src} of the order of several λ, the waveguide aperture provides indeed a good approximation to a point source. The average full width at half maximum (FWHM) of the profiles at $d_{\mathrm{focus}}\approx 8\lambda$ depicted in Fig. 6 is $1.60a\approx 1.08\lambda$, on par with λ. We alert the reader that a subwavelength focusing as discussed in recent studies[16] is not concerned here. The subwavelength focusing requires the amplification of evanescent waves through the photonic crystal for image formation. This implies an upper limit on the location of the source and image from the PC, since the evanescent waves decay rapidly away from the interfaces.

Similar to the lateral shift, the shift of the source along the longitudinal direction is expected to be followed by the focus pattern. The FDTD simulated 2D map of the magnetic field,

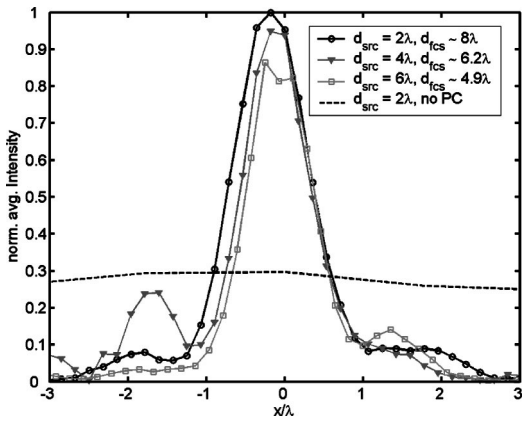

FIG. 8. The measured lateral intensity profiles at respective focal distances for different source distances. The intensity axis is normalized by the $d_{\mathrm{src}}=2.0\lambda$ profile peak. The dashed line denotes the intensity profile in the absence of PC for $d_{\mathrm{src}}=2\lambda$.

$H_y(x,z)$, plotted in Fig. 7 shows this behavior clearly: When the source is moved from $d_{src}=2\lambda$ to $d_{src}=4\lambda$ away, the focus pattern on the other side shifts accordingly towards the PC-air interface.

In Fig. 8, the measured lateral profiles at focus points for various d_{src} are plotted. From the determined focal positions we have found that $(d_{src}+d_{focus})$ remains roughly constant. The figure also displays the intensity profile in the absence of the PC for $d_{src}=2\lambda$ case (dotted line). At the focal distance, the free space propagation is almost a flat line with no features indicating the source location. The intensity achieved by the PC is ~12 dB higher relative to freespace propagation at the focal distance.

IV. CONCLUSION

In this article, the negative refraction and the point focusing analysis of a 2D hexagonal dielectric photonic crystal is presented. The TE polarized fifth band of the crystal is demonstrated to exhibit negative refraction for a plane wave source, and focusing for an omni-directional source. Flat lens behavior is achieved for arbitrary source positions. We finally note that the focusing effect reported in this article depends only on the refractive index of the dielectric material and on the geometrical parameters of the 2D PC, hence it should be scalable to optical wavelengths. Indeed, such focusing behavior is reported at infrared wavelengths very recently.[20]

ACKNOWLEDGMENTS

This work was supported by EU-DALHM, DARPA contract MDA 972-01-2-0016, and EU-METAMORPHOSE NATO. Ames Laboratory is operated for the U. S. Department of Energy by Iowa State University under Contract No. W-7405-Eng-82.

*Corresponding author. Email address: guven@fen.bilkent.edu.tr

[1] J. D. Joannopoulos, R. D. Meade, and J. N. Winn, *Photonic Crystals: Molding the Flow of Light* (Princeton University Press, Princeton, NJ, 1995).
[2] H. Kosaka, T. Kawashima, A. Tomita, M. Notomi, T. Tamamura, T. Sato, and S. Kawakami, Phys. Rev. B **58**, R10096 (1998).
[3] B. Gralak, S. Enoch, and G. Tayeb, J. Opt. Soc. Am. A **17**, 1012 (2000).
[4] M. Notomi, Phys. Rev. B **62**, 10696 (2000).
[5] C. Luo, S. G. Johnson, J. D. Joannopoulos, and J. B. Pendry, Phys. Rev. B **65**, 201104 (2002).
[6] S. Foteinopoulou, E. N. Economou, and C. M. Soukoulis, Phys. Rev. Lett. **90**, 107402 (2003).
[7] S. Foteinopoulou and C. M. Soukoulis, Phys. Rev. B **67**, 235107 (2003).
[8] E. Cubukcu, K. Aydin, E. Ozbay, S. Foteinopoulou, and C. M. Soukoulis, Nature (London) **423**, 604 (2003).
[9] E. Cubukcu, K. Aydin, E. Ozbay, S. Foteinopoulou, and C. M. Soukoulis, Phys. Rev. Lett. **91**, 207401 (2003).
[10] P. V. Parimi, W. T. Lu, P. Vodo, and S. Sridhar, Nature (London) **426**, 404 (2003).
[11] P. V. Parimi, W. T. Lu, P. Vodo, J. Sokoloff, J. S. Derov, and S. Sridhar, Phys. Rev. Lett. **92**, 127401 (2004).
[12] D. R. Smith, W. J. Padilla, D. C. Vier, S. C. Nemat-Nasser, and S. Schultz, Phys. Rev. Lett. **84**, 4184 (2000).
[13] R. A. Shelby, D. R. Smith, and S. Schultz, Science **292**, 77 (2001).
[14] V. G. Veselago, Usp. Fiz. Nauk **92**, 517 (1964) [Sov. Phys. Usp. **10**, 509 (1968)].
[15] J. B. Pendry, Phys. Rev. Lett. **85**, 3966 (2000).
[16] C. Luo, S. G. Johnson, J. D. Joannopoulos, and J. B. Pendry, Phys. Rev. B **68**, 045115 (2003).
[17] A. Martínez, H. Míguez, A. Griol, and J. Martí, Phys. Rev. B **69**, 165119 (2004).
[18] S. Foteinopoulou and C. M. Soukoulis, cond-mat/0403542 (unpublished).
[19] Zhi-Yuan Li and Lan-Lan Lin, Phys. Rev. B **68**, 245110 (2003).
[20] A. Berrier, M. Mullot, M. Swillo, M. Qiu, L. Thylén, A. Talneau, and S. Anand, Phys. Rev. Lett. **93**, 073902 (2004).